Analytical Biochemistry 501 (2016) 26–34

Contents lists available at ScienceDirect

Analytical Biochemistry

journal homepage: www.elsevier.com/locate/yabio

A simple and accurate protocol for absolute polar metabolite quantification in cell cultures using quantitative nuclear magnetic resonance

Luca Goldoni [a, *], Tiziana Beringhelli [b], Walter Rocchia [c], Natalia Realini [a], Daniele Piomelli [a, d]

[a] Drug Discovery and Development, Istituto Italiano di Tecnologia, 16163, Genova, Italy
[b] Department of Chemistry, University of Milan, 20133, Milano, Italy
[c] CONCEPT Lab, Istituto Italiano di Tecnologia, 16163, Genova, Italy
[d] Departments of Anatomy and Neurobiology, Pharmacology, and Biological Chemistry, University of California, Irvine, CA, 92697, USA

ARTICLE INFO

Article history:
Received 8 October 2015
Received in revised form
8 February 2016
Accepted 9 February 2016
Available online 18 February 2016

Keywords:
^{1}H-NMR
pH-controlled serum removal
PULCON
Accuracy
CPMG
Deconvolution

ABSTRACT

Absolute analyte quantification by nuclear magnetic resonance (NMR) spectroscopy is rarely pursued in metabolomics, even though this would allow researchers to compare results obtained using different techniques. Here we report on a new protocol that permits, after pH-controlled serum protein removal, the sensitive quantification (limit of detection [LOD] = 5–25 μM) of hydrophilic nutrients and metabolites in the extracellular medium of cells in cultures. The method does not require the use of databases and uses PULCON (pulse length-based concentration determination) quantitative NMR to obtain results that are significantly more accurate and reproducible than those obtained by CPMG (Carr–Purcell–Meiboom–Gill) sequence or post-processing filtering approaches. Three practical applications of the method highlight its flexibility under different cell culture conditions. We identified and quantified (i) metabolic differences between genetically engineered human cell lines, (ii) alterations in cellular metabolism induced by differentiation of mouse myoblasts into myotubes, and (iii) metabolic changes caused by activation of neurotransmitter receptors in mouse myoblasts. Thus, the new protocol offers an easily implementable, efficient, and versatile tool for the investigation of cellular metabolism and signal transduction.

Interest in quantitative nuclear magnetic resonance (*q*-NMR) analysis has steadily increased since the seminal works of Jungnickel and Forbes [1] and Hollis [2], owing to the unique ability of this methodological approach to quantify, at the same time, a wide range of structurally diverse biological substances with high throughput and automation [3]. Compared with other analytical techniques, *q*-NMR does not require chromatographic separation, generates signals that are directly proportional to the number of NMR-active nuclei in the targeted analyte [4,5], and offers a high degree of assay reproducibility [6] along with reduced uncertainty [7,8]. Moreover, advances in hardware development—such as the introduction of high-field magnets and cryogenic probes—have progressively lowered the limit of detection (LOD) for analytes, thereby improving the overall sensitivity of the technique [4].

The PULCON (pulse length-based concentration determination) procedure [9], one of the most promising methods for *q*-NMR [4], finds its mathematical and physical foundation in the principle of reciprocity [10–12]. This principle states that the strength of a signal is inversely proportional to the 90° pulse length in the active volume of the NMR tube. The PULCON method can be implemented in all types of commercial NMR spectrometers and requires only one

Abbreviations used: *q*-NMR, quantitative nuclear magnetic resonance; LOD, limit of detection; PULCON, pulse length-based concentration determination; CPMG, Carr–Purcell–Meiboom–Gill; D_2O, deuterium oxide; DMS, dimethylsulfone; DMEM, Dulbecco's modified Eagle's medium; TSP, 3-(trimethylsilyl)propionic-2,2,3,3-d_4 acid sodium salt; PBS, phosphate buffer solution; DM, differentiation medium; TFA, trifluoroacetic acid; 1D, one-dimensional; NOESY, nuclear Overhauser effect spectroscopy; 2D, two-dimensional; FID, free induction decay; COSY, correlation spectroscopy; TOCSY, total correlation spectroscopy; HSQC, heteronuclear single quantum coherence; ANOVA, analysis of variance; S/N, signal/noise; LOQ, limit of quantification; AC, acid ceramidase; NAAA, *N*-acylethanolamine acid amidase.

* Corresponding author.
E-mail address: luca.goldoni@iit.it (L. Goldoni).

http://dx.doi.org/10.1016/j.ab.2016.02.009
0003-2697/

reference spectrum that, thanks to the stability of modern NMR instruments, can be used for several months [9]. Furthermore, using an external standard, it allows virtually complete sample recovery. PULCON has been recently validated for quantification of natural product [13,14] in the millimolar range of concentrations. Despite its potential, PULCON has yet to be validated for complex biological matrices, such as media of cultured cells, in which NMR analysis is hindered by the presence of interfering proteins. Strategies commonly used to overcome such interference are applied in either the data acquisition step, using the Carr–Purcell–Meiboom–Gill (CPMG) sequence, or dedicated algorithms in the post-processing step. A possible alternative is to physically remove proteins from biological matrices, as was recently reported [15–17]. Unfortunately, in cell cultures the efficiency of the methods commonly used for protein removal is strongly limited by the variability of the medium pH.

In the current article, we describe a new and efficient protocol based on PULCON *q*-NMR that, after pH-controlled removal of serum proteins, allows for the sensitive quantification (LOD = 5–25 μM) of the principal hydrophilic nutrients and metabolites found in the extracellular medium of mammalian cells in cultures without the use of commercial databases [18]. Using a newly devised figure of merit, we show that the method is substantially more reproducible and accurate than the methods reported previously. Furthermore, we provide three applications of the method that illustrate its flexibility: (i) identification of metabolic differences between genetically engineered human cells lines, (ii) alteration in cellular metabolism induced by differentiation of mouse myoblasts into myotubes, and (iii) metabolic changes resulting from pharmacological interventions targeting cell surface receptors. The new protocol offers an efficient, accurate, versatile, and inexpensive tool for the investigation of cellular metabolism and signal transduction.

Materials and methods

Methanol, acetonitrile, deuterium oxide (D_2O), monobasic (KH_2PO_4) and dibasic (K_2HPO_4) potassium phosphate, dimethylsulfone (DMS), Dulbecco's modified Eagle's medium (DMEM), and 3-(trimethylsilyl)propionic-2,2,3,3-d_4 acid sodium salt (TSP) were obtained from Sigma–Aldrich (Milan, Italy).

Standard solutions of DMS for PULCON calibration (and for accuracy and precision measurements) were freshly prepared from powder dissolved in 100 mM potassium phosphate/D_2O buffer (pH 7.15) containing TSP as reference. Independent weights of approximately 5–10 mg each were made by an analytical balance (Mettler Toledo XP205, certified uncertainty = 0.013 mg) and brought to volume in 5-ml volumetric flasks. DMEM solutions were obtained by serial dilutions of a standard stock of 2× DMEM freshly prepared from powder dissolved in MilliQ water.

Cell cultures

Wild-type human embryonic kidney cells (Hek293-WT) were purchased from American Type Culture Collection (Manassas, VA, USA). Heck293-WT cells, Hek293 cells overexpressing *h*AC1 (Hek293-*h*AC1) [19], and Hek293 cells overexpressing human NAAA (Hek293-*h*NAAA) [20] were plated in 150-mm dishes (5×10^6 cells/dish) and cultured in complete DMEM containing 10% fetal bovine serum, 2 mM L-glutamine, and antibiotics (100 U/ml penicillin and streptomycin) at 37 °C and 5% CO_2. Cell media were collected 48 h after incubation. Cells were washed with phosphate buffer solution (PBS), detached with trypsin, and counted using a Scepter 2.0 Cell Counter (Millipore, Milan, Italy). Absolute metabolite concentrations were normalized to cell counts. Pharmacological treatment with 3-bromopyruvic acid was performed for 18 h at 25 or 50 μM. Murine C2C12 cells were a gift from Maria Pennuto (Istituto Italiano di Tecnologia, IIT) and were grown in complete DMEM at 37 °C and 5% CO_2. Cells were differentiated into myotubes as follows: they were seeded in 35-mm dishes at 250×10^3 cells/dish, and normal medium was substituted with DMEM containing 2% horse serum, 100 U/ml penicillin, and streptomycin (differentiation medium, DM). To obtain myotubes, cells were cultured for 9 days in DM. Samples of culture medium were collected every 3 days for analysis. Absolute metabolite concentrations were normalized to protein content. Carbachol was dissolved in DMEM (2 mM) and added to culture medium at different concentrations (50 or 100 μM). Cell medium was replaced every 24 h for a total period of 72 h.

The freeze-drying process

First, 400 μl of the medium (DMEM, DMEM–serum, and DMEM–serum after cell culture) were transferred to a 15-ml Falcon tube. Solutions were frozen in liquid N_2 and freeze-dried for at least 3 h until the formation of a fluffy solid. The powder was reconstituted in deuterated buffer for NMR analysis.

Protein serum removal methods

Various conditions for protein serum removal were tested (see Table 1 in Ref. [21]), applying the following general scheme: an appropriate volume of ice-cold precipitation solvent (methanol or acetonitrile) was added to 400 μl of DMEM–serum on ice, and the solution was stirred for 20 s, incubated for 20 min, and centrifuged at 2100 rcf (relative centrifugal force) for 15 min at 4 °C. The supernatants were collected, diluted with 3.4 ml of water, freeze-dried for at least 12 h until the formation of a fluffy solid, and reconstituted in 0.4 ml of deuterated buffer. The most efficient serum protein removal for DMEM–serum solution was achieved by adding trifluoroacetic acid (TFA) up to pH 6 and cold methanol (1.2 ml) (3:1). After cell cultures, the pH was adjusted to 6 by adding sodium hydroxide (NaOH) or TFA.

NMR spectroscopy

NMR experiments were performed without spinning on a Bruker Avance III 600-MHz spectrometer equipped with a 5-mm QCI cryoprobe with *z* shielded pulsed-field gradient coil. In the experiments, 3-mm tubes (Norell, SVCP-3-103.5-96PK) filled with 300 μl of the sample solutions were used. Before each acquisition, automatic matching and tuning were run, the 90° pulse was optimized by means of an automatic pulse calculation routine [22], and the homogeneity was automatically adjusted on each sample tube. Before data acquisition, the samples were equilibrated for 2 min inside the probe and the temperature was actively controlled at 298 K. In all *q*-NMR experiments, 32 transients were accumulated, at a fixed receiver gain, using 65,536 complex data points over a spectral width of 20.6 ppm and with a relaxation delay of 30 s (more than 5 times the longest T_1 of the analytes; see Table S1 in online supplementary material). A power level of 1.706 e^{-5} W was employed for pre-saturation in one-dimensional (1D)–NOESY (nuclear Overhauser effect spectroscopy) "presat" experiment, whereas interpulse spacings and a duty cycles were 2.3 ms and 20 for 1D–CPMG or 0.12 ms and up to 1200 for T_2 measurements through 2D-CPMG. An exponential line broadening (0.1 Hz) was applied to FIDs (free induction decays) before Fourier transform. The spectra were manually phased and automatically baseline corrected (as preferred in metabolomics [4]). A bias and slope manual correction of the integrals was applied only when signals were close or overlapped at the peak base. Typically, 2D

Table 1
Accuracy and precision of measurements at different theoretical concentrations.

Theoretical concentration (mM)[a]	Mean measured concentration (mM)[a]	Accuracy (%)	Relative standard deviation (%)
7.3000	7.3400	0.55	0.59
5.0000	5.0141	0.28	0.17
0.7300	0.7306	0.09	1.52
0.5000	0.4970	0.61	0.72
0.0730	0.0722	1.10	0.86
0.0500	0.0494	1.21	1.71
0.0250	0.0245	1.87	1.01
0.0073	0.0074	0.91	0.79
0.0050	0.0051	2.00	4.00

[a] The decimal digits reported correspond to the precision of the analytical balance, which allows for a concentration precision greater than $2e^{-5}$ mM. The inter-sample reproducibility is assessed by the percentage relative standard deviation reported in the fourth column.

experiments were performed as follows. $^{1}H-^{1}H$ COSY(correlation spectroscopy): 64 FIDs, 1024 data points, 128 increments, spectral width of 10 ppm for both dimensions with the transmitter frequency offset at 4.6 ppm; the residual water signal was pre-saturated with continuous wave pre-saturation during the 2-s relaxation delay. $^{1}H-^{1}H$ TOCSY (total correlation spectroscopy): 32 FIDs, 1024 data points, 256 increments, spectra widths of 10 ppm for both dimensions with the transmitter offset at 4.6 ppm, mixing time of 80 ms, and relaxation delay of 1.8 s. $^{1}H-^{13}C$ HSQC (heteronuclear single quantum coherence) and edited $^{1}H-^{13}C$ HSQC (multiplicity edited HSQC that returns cross-peaks with opposite phases for CH_2 and CH/CH_3): 96 FIDs, 1024 data points, 256 increments, $^{1}J_{CH} = 145$ Hz, spectral width of 10 ppm for ^{1}H and 165 ppm for ^{13}C (transmitter frequency offsets at 4.6 and 75 ppm, respectively).

Statistics

All statistical analyses were performed with Prism software 5.03 (GraphPad Software, San Diego, CA, USA). Nutrient/catabolite concentrations are expressed as means ± standard errors. Differences between cell types were analyzed using a Student's *t* test or one-way analysis of variance (ANOVA) followed by pairwise Tukey's multiple post hoc test. Two-way ANOVA followed by Bonferroni's post hoc test was used to study drug treatments on different cell types, whereas one-way ANOVA followed by Dunnett's multiple comparison post hoc test was employed to study drug treatments on a single cell type. The level of statistical significance was set at $P < 0.05$ for Bonferroni's test. Differences between groups were considered statistically significant for values of $P < 0.05$.

Results and discussion

Method validation

In a first set of experiments, we asked whether PULCON *q*-NMR might be used accurately to quantify micromolar concentrations of DMS, a standard for *q*-NMR. PULCON standard reference signal for calibration was provided by a freshly prepared 10-mM DMS solution. Before each series of acquisitions, a system suitability test [23] was performed on the calibration solution to assess specificity and sensitivity of the spectrometer. Acceptance criteria were the following: line width at half-height of a singlet DMS signal <1.5 Hz, percentage relative standard deviation (STD %) ≤4 in the dynamic range of 10^3, and difference in chemical shift <0.2 Hz. PULCON calibration (see Eq. S1 in supplementary material) and system suitability tests are compulsory at each cycle of warm-up and cool-down of the cryoprobe, mainly owing to small variations in temperature coil. The accuracy was evaluated by measuring the concentration of nine standard solutions obtained by serial dilutions from 5- and 7.3-mM freshly prepared DMS solutions. The samples were prepared and tested in triplicate for an estimate of measurement precision. Results are reported in Table 1.

The greatest error (2%) and highest imprecision in the measurements (4%) were observed at the lowest concentration of DMS (0.005 mM). Even at that low concentration, however, the signal/noise (S/N) ratio was larger than 7. We infer, therefore, that over a dynamic range $>10^3$, the overall absolute relative error remains lower than 2%, in agreement with the work of Burton and coworkers [13,24]. Even though PULCON *q*-NMR is linear by definition (Eq. S1), linearity was controlled by plotting the average measured concentration (three replicates) versus the theoretical concentration. Fitting the experimental data by least-squares linear regression resulted in the following equation: $y = 1.0049x - 0.0019$ ($R^2 = 0.99998$, squared correlation coefficient), indicating excellent data linearity.

In NMR spectroscopy, in principle, the S/N ratio (and therefore the LOD and limit of quantification [LOQ]) [25] can be improved by increasing the number of transients, but in the current case the number of transients was the same for all of the analyzed samples. The LOD and LOQ can be calculated by the standard deviation of the response σ and the slope S of the linear regression using the lowest values of concentration, close to zero, assuming as confidence levels 3.3σ for the LOD and 10σ for the LOQ, as described by the following formula [23]:

$$\mathrm{LOD} = 3.3\sigma/S \text{ and } \mathrm{LOQ} = 10\sigma/S, \quad (1)$$

where σ is the standard deviation of the response (i.e., the square root of the sum of the squared distance of each measurement point from the linear regression line, divided for $n - 1$ points, used for linear regression fitting) and S is the slope of the regression line. The (not mediated) data obtained from the concentration range 5–70 μM, previously exploited for the linearity test, were subjected to a new least-squares linear regression. The returned equation was $y = 0.9868x + 0.0506$ ($R^2 = 0.9997$). For the ^{1}H quantitative experiment, we found an LOD of 1.46 μM and an LOQ of 4.42 μM.

To address the issue of possible matrix effect, we selected DMEM as a model (Fig. 1). PULCON *q*-NMR was validated through the absolute quantification of DMEM components in five solutions obtained by serial dilutions of a freshly prepared standard 2× solution. 2D experiments ($^{1}H-^{1}H$ COSY, $^{1}H-^{1}H$ TOCSY, $^{1}H-^{13}C$ HSQC, and edited $^{1}H-^{13}C$ HSQC) provided preliminary identification of DMEM components, an essential step to ensure the specificity of the analytical procedure and allow quantification of the components even in the presence of interfering factors (e.g., impurities, decomposition product, matrix components) [26]. The unambiguous assignment of every resonance in each analyte was achieved, and the results were compared with ^{1}H and ^{13}C values reported for each analyte in the Amix, Bruker database (Fig. 1).

Of the 15 components identified in DMEM, the majority (13) were quantifiable. However, to guarantee selectivity, we quantified only

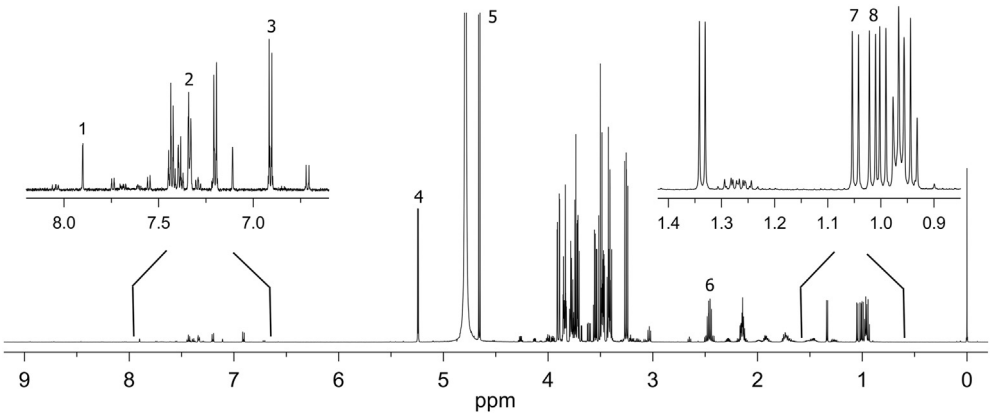

Fig.1. ^{1}H q-NMR spectrum of 2× DMEM in the deuterated buffer: (1) histidine; (2) phenylalanine; (3) tyrosine; (4) α-glucose; (5) β-glucose; (6) glutamine; (7) valine; (8) isoleucine.

nutrients showing at least one signal with low spin multiplicity, not overlapping with other resonances, measurable without interference from other components of the mixture [26], and with concentrations > LOQ (for at least four of the five solutions) (Table 2).

A freeze-drying step was introduced to avoid the use of solvent suppression techniques, which may cause partial saturation of exchangeable analyte protons as well as of signals that are close in frequency to solvent signals (e.g., the anomeric β-glucose proton; see Fig. S1 in supplementary material). After the freeze-drying step, the powder was reconstituted in deuterated buffer for NMR analysis to avoid signals shift and peak broadening due to residual acidity. The concentration of analytes obtained after lyophilization was identical to theoretical values, within the inaccuracy of the PULCON method. By contrast, as expected [4], inaccuracy was higher, especially for the β-glucose signal, when solvent suppression was used (see Table S2 in supplementary material).

Response linearity was assessed plotting average analyte concentrations versus theoretical values. R^2 values for most analytes were > 0.9999 and never lower than 0.9998, (Table 2). The maximum deviation of the slope from the ideal value of 1 that accounts for the inaccuracy of the PULCON method was 1.64% (valine). The method reproducibility was further tested by measuring analyte concentrations in new freshly prepared DMEM samples using, as external standard reference, a DMS spectrum acquired 1 year earlier. R^2 was always >0.9986, with the largest discrepancy between the slopes (S) within 0.88% (Table 2). These values are comparable to those reported by Holzgrabe and coworkers for other q-NMR methods [27].

The serum issue in q-NMR

An additional challenge in metabolomics analysis of cells in cultures is the presence of serum. Serum contains substantial amounts of proteins that produce broad interfering signals (Fig. 2A). Such signals can affect the baseline in ^{1}H NMR spectra, resulting in an overestimation of the concentrations of all the metabolites (see Table 2 in Ref. [21]) except anomeric protons of α-glucose and β-glucose, whose signals are in a spectral region with no interference from protein signals (see Fig. S1). Model solutions were prepared by the addition of bovine serum (10%) to DMEM solutions.

One of the strategies to overcome the problem of overestimation is using a CPMG spin–echo sequence, $90–[(\tau–180–\tau)_n]$, for data acquisition. An accurate choice of the parameters τ (evolution time) and n (echo repetitions) allows for the suppression of protein signals exploiting the large difference between the very short T_2 (transverse) relaxation times of hydrogen atoms belonging to high molecular weight molecules and those (longer) of hydrogen atoms belonging to small molecule such as nutrients and metabolites [28]. However, this procedure is neither straightforward nor flawless. First, proteins can bind many small molecules such as citrate, lactate, aromatic amino acid, and metabolites, shortening their relaxation time T_2 to that of the protein. Hence, the use of CPMG [29], optimized for the protein signal filtering, leads (in the most favorable cases) to underestimating the concentrations of some small molecules or (in the worst cases) to completely missing the analyte (e.g., seeing the phenol red). Indeed, phenol red signal, a sharp doublet at 6.7 ppm in DMEM without serum (Fig. 1), in the presence of serum, is so broad (with the same T_2 time of the protein) to be undetectable (Fig. 2A) and lost by CPMG filtering (Fig. 2B). Second, to correlate the signal intensities measured by the 1D–CPMG experiment to the concentration of the molecules to which they belong, the signal decay due to its intrinsic T_2 should be considered. Therefore, the 1D–CPMG signal intensities should be corrected as follows:

$$I_0 = I_x \exp(2\tau n/T_2), \tag{2}$$

Table 2
Range of concentrations measured of DMEM nutrients, square correlation coefficient (R^2), slope (S), and ordinate intercept (b) of least squares regression line.

Nutrient	Concentration range (mM)	R^2	S	b	Reproducibility		
					R^2	S	b
α-Glucose	17.9152–0.9084	1.0000	0.9994	+0.0189	1.0000	0.9919	−0.0251
β-Glucose	30.7454–1.5684	1.0000	1.0024	−0.0723	1.0000	0.9952	−0.0113
Histidine	0.3777–0.0464	0.9998	1.0162	−0.0035	0.9988	0.9937	−0.0036
Phenylalanine	0.8398–0.1040	0.9999	1.0003	−0.0009	1.0000	0.9940	−0.0005
Tyrosine	0.7516–0.0338	0.9999	1.0055	−0.0044	0.9999	0.9982	−0.0018
Glutamine	7.5753–0.3932	1.0000	1.0007	+0.0037	1.0000	0.9927	+0.0105
Isoleucine	1.5782–0.0766	1.0000	1.0014	+0.0044	0.9997	0.9912	−0.0077
Valine	1.5610–0.0740	1.0000	0.9836	−0.0046	0.9986	0.9977	−0.0163

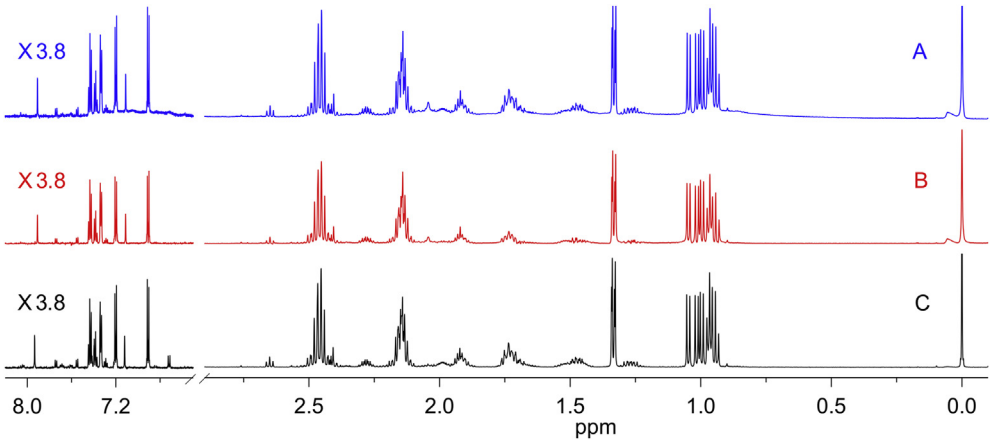

Fig.2. ^{1}H spectra of 2× DMEM with 10% of serum: (A) *q*-NMR; (B) *q*-NMR 1D–CPMG; (C) *q*-NMR after serum removal.

where I_0 is the signal intensity after the 90° pulse before evolution, I_x is the measured intensity after τ evolution, and T_2 is the transverse relaxation time. Thus, the knowledge of T_2 is required for each metabolite. Further T_2 determination or the quantification of multiplets can be seriously affected by J-modulation. In spite of the many strategies proposed to overcome these problems [30], the CPMG method for absolute metabolites concentration measurement is anything but straightforward and not readily applicable to high-throughput analyses such as those conducted in metabolomics studies.

A possible alternative consists in acquiring the simple ^{1}H *q*-NMR of medium and subsequently removing the contribution of broad protein signals to the integrated intensities of signals of interest using a post-processing background removal method. We tested two different software tools; the first one is completely automated, whereas the second one allows the analyst to manually select the fitting area and the integral adjustment of the peaks. The first software we examined (Assure 1.5, Bruker) exploits a baseline-filtering algorithm that eliminates all of the signals broader than a given line width. We set such upper limit at 10–15 Hz, achieving a satisfactory removal of the protein background without reduction of the measured area of the sharp signals. Once tuned for each spectral region, the baseline filtering routine works in automation and has a relevant and reliable throughput irrespective of operator experience (see Table 2 in Ref. [21]). The second software we examined relies on a line-fitting algorithm (MestReNova 6.0). A region of the NMR spectrum is deconvoluted into some of its component peaks (using a suitable percentage of Lorentzian and Gaussian characters), creating an artificial spectrum as a sum of each component, where the protein signals are not added. The software is easy to run, is interactive, and provides the fitting error (see Table 2 in Ref. [21]).

A third option is to physically remove the serum from the biological matrix before measuring metabolite concentrations. We pursued this option testing different serum removal conditions (see Table 1 in Ref. [21]). The best condition in terms of minimization of protein signals, reproducibility, and recovery was found by using cold methanol (methanol/DMEM–serum, 3:1, v/v) (see Figs. 1 and 2 in Ref. [21]) in combination with pH adjustment by the addition of TFA. pH control was essential because no protein precipitation was observed at pH values above 8 or below 3, only partial precipitation occurred at pH values of 7 and 4, whereas optimal precipitation conditions were found at pH 6 (see Fig. 3 in Ref. [21]). Even though deproteinization methods are widely described in the literature [16,29], to the best of our knowledge, the impact of pH control has never been examined before. This issue is extremely relevant in cell cultures where the pH of the medium ranges from 8.5 of fresh DMEM–serum down to acidic (pH 3–4) after cell culture, mainly due to the release of lactic acid in the medium. Furthermore, the pH-controlled serum removal causes the release of analytes bound to proteins, as can be inferred from the signal of the phenol red at 6.7 ppm (Fig. 2C), which returns to be a sharp doublet, after serum removal, as it was in DMEM without serum (Fig. 1). This is likely due to unfolding and precipitation of serum proteins. Measured analyte concentrations were then compared with theoretical values (see Table 2 in Ref. [21]). Such single point differences (e.g., for α-glucose maximum of ~7%) might not be the most appropriate for the estimation of nutrients loss because they are affected by multiple and intermingled error sources, including the measurement process error. Therefore, for each analyte we performed a linear least-squares fitting of the concentrations measured in the five DMEM–serum solutions after serum removal (average of three replicates) versus their respective theoretical concentrations. The deviations of the obtained slopes from the ideal value of 1 provide a better estimate of the overall inaccuracy for each analyte. As reported in Table 3, the maximum deviation of the obtained slopes was found to be less than 5.7% (α-glucose, β-glucose, and isoleucine), whereas R^2 values were never lower than 0.9993. The PULCON inaccuracy, independently estimated, is 1.64%. Then, for each analyte, an estimate of the nutrient loss due to the removal process can be inferred accordingly.

Moreover, separate measurements on freshly prepared solutions confirmed the high reproducibility of the overall process, $R^2 > 0.9993$ and a deviation of $S \leq 6.1\%$ (α-glucose).

The ability of methanol to precipitate proteins and pH precipitation dependence was also tested in the presence of greater amounts of serum (up to 80%). Optimal protein removal was confirmed to occur at pH 6 irrespective of serum levels (see Fig. 4 in Ref. [21]).

Method comparison

The quantitative results obtained on the five model solutions after protein removal were compared with those obtained without protein removal (i) directly on the rough freeze-dried/reconstituted solutions, (ii) using the CPMG acquisition scheme, and (iii) applying post-processing filtering procedures. The acquisition and processing of all the spectra were performed by a single operator and in the most standardized way (one laboratory, many methods [31]). Although R^2 accounts for the precision of the measurement process, a different criterion should be adopted to assess the accuracy of the methods previously considered for removing the signal of the

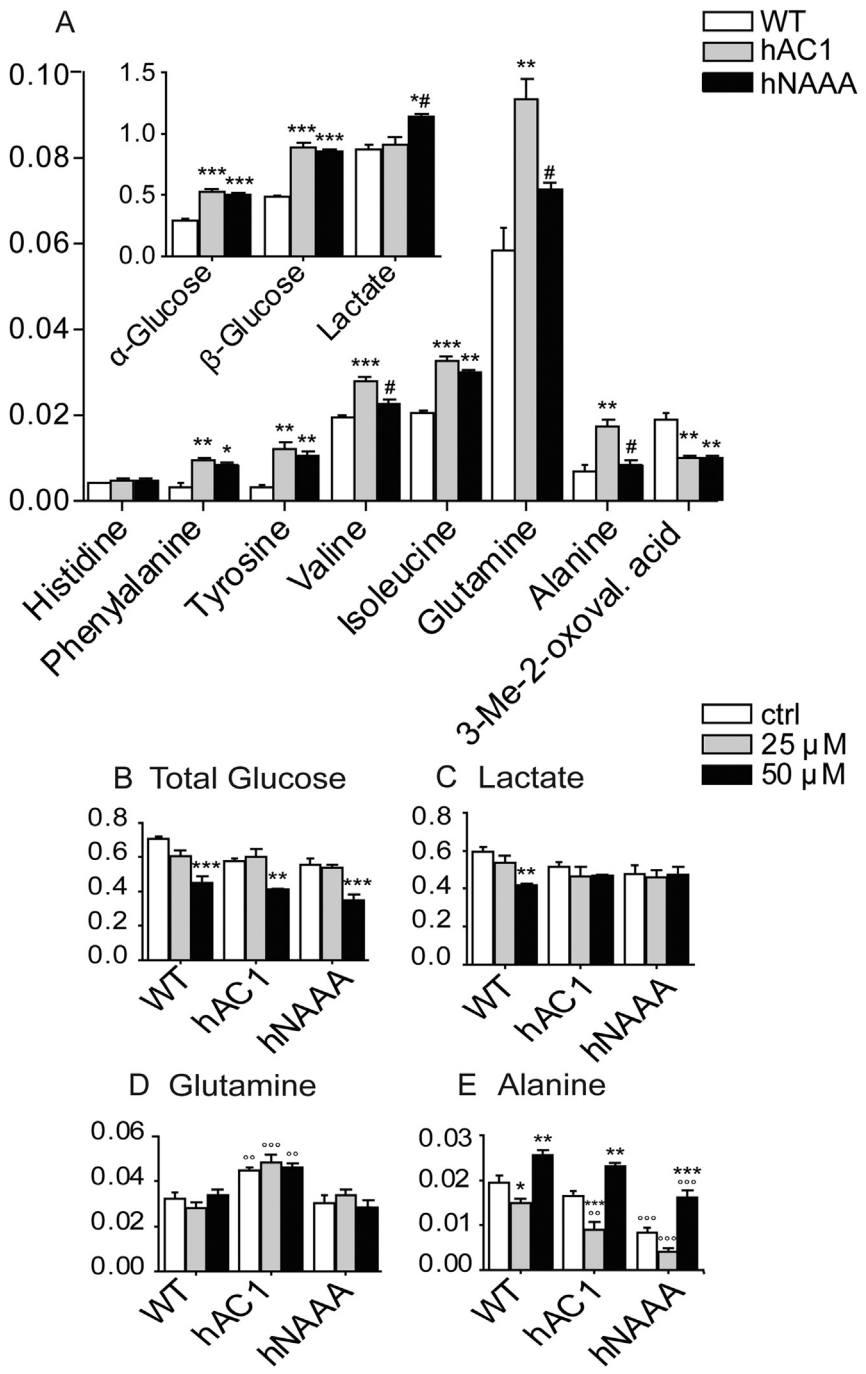

Fig.3. (A) HeK293—WT, HeK293—*h*AC1, and HeK293—*h*NAAA absolute concentration of nutrient uptake and catabolites (mM) normalized to cell number (millions of cells). For nutrients (glucose, histidine, phenylalanine, tyrosine, valine, isoleucine, and glutamine), the absolute value of the difference between the amount measured in cell culture medium and the amount of same nutrient in DMEM without cells is reported. The concentrations of catabolites (lactate, alanine, and 3-methyl-2-oxovaleric acid [3-Me-2-oxoval. acid]) are reported as measured in cell culture medium. One-way ANOVA followed by all pairwise Tukey's multiple comparison test: $^{***}P < 0.001$, $^{**}P < 0.01$, and $^{*}P < 0.05$ versus Hek293-WT; $\#P < 0.05$ versus Hek—*h*AC1. Effect of 3-bromopyruvic acid treatment at doses of 25 and 50 µM analyzed by two-way ANOVA. (B) Total glucose uptake: cell type, $F(2, 27) = 9.346$, $P = 0.0008$; treatment, $F(2, 27) = 41.59$, $P < 0.0001$. (C) Lactate release: treatment, $F(2, 27) = 3.692$, $P = 0.0383$. (D) Glutamine uptake: cell type, $F(2, 27) = 31.46$, $P < 0.0001$. (E) Alanine release: cell type, $F(2, 27) = 55.52$, $P < 0.0001$; treatment, $F(2, 27) = 75.65$, $P < 0.0001$. Bonferroni post hoc test versus control group (ctrl): $^{***}P < 0.001$, $^{**}P < 0.01$, and $^{*}P < 0.05$. Bonferroni post hoc test versus Hek293—WT: $^{\circ\circ\circ}P < 0.001$ and $^{\circ\circ}P < 0.01$. The level of statistical significance was set at $P < 0.05$. Results are expressed as means ± standard errors ($n = 3$–4). Experiments were repeated twice with similar results.

proteins present in the serum. For this purpose, we used the following figure of merit:

$$a = (S - 1)^2 + (b/MTCV)^2. \quad (3)$$

Because our purpose was to evaluate the performance of various protocols, we considered in our figure of merit not only the slope S of the regression line but also the ordinate intercept b. This value was normalized by the minimum theoretical concentration value ($MTCV$) considered on each analyte in order to compensate for the high sensitivity of b to the different concentration ranges for the various analytes and, in particular, to the distance from the origin.

Table 3
Range of concentrations measured of DMEM nutrients, square correlation coefficient (R^2), slope (S), and ordinate intercept (b) of least squares regression line.

Nutrient	Range of concentration (mM)	R^2	S	b	Independent solutions		
					R^2	S	b
α-Glucose	15.3975–0.8087	0.9999	0.9432	−0.0030	0.9993	0.9389	+0.0170
β-Glucose	26.5280–1.4403	0.9999	0.9438	+0.0964	0.9994	0.9616	+0.0255
Histidine	0.3294–0.0422	0.9997	0.9626	−0.0015	0.9990	0.9607	+0.0021
Phenylalanine	0.7456–0.0926	0.9993	0.9852	−0.0041	0.9996	0.9457	+0.0061
Tyrosine	0.6692–0.0378	0.9998	0.9792	−0.0002	0.9998	0.9511	+0.0008
Glutamine	6.6608–0.3432	1.0000	0.9668	−0.0032	0.9998	0.9455	+0.0046
Isoleucine	1.3293–0.0715	0.9997	0.9492	+0.0029	0.9997	0.9450	−0.0001
Valine	1.3681–0.0740	0.9997	0.9781	−0.0001	0.9998	0.9405	+0.0082

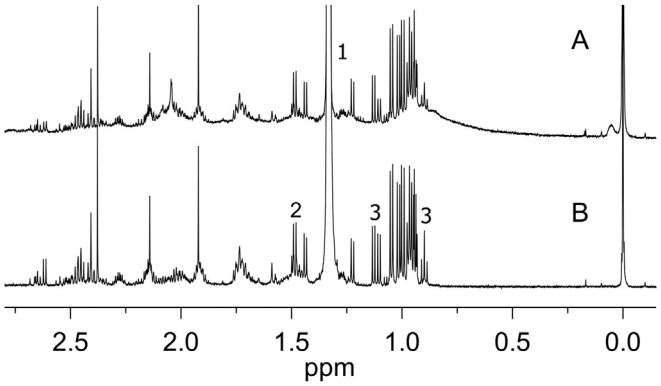

Fig.4. ^{1}H q-NMR spectrum of the medium after cell culture (Hek293–WT at 48 h): (A) with serum; (B) with serum removed. The following metabolites released in the medium have been identified: (1) lactate; (2) alanine; (3) 3-methyl-2-oxovaleric acid.

In ideal conditions, the measured and theoretical concentrations are equal; thus, $S = 1$ and $b = 0$. Therefore, the lower the value of a is, the closer to real values the measurements are. The pH-controlled protein removal method, in addition to providing a greater precision than all other methods ($R^2 > 0.9993$, mean value of 0.9998 vs. 0.9979–0.9988; Table 4) also provides significantly improved accuracy considering both each individual analyte and the overall components. Indeed, the mean value of the parameter a is two orders of magnitude lower than the best of the other methods. Even normalizing the b value by the average theoretical concentration (see Table S3 in supplementary material), the mean value of the a parameter for protein removal method still remains more than 5 times smaller than the best value obtained for all of the other methods.

This is in agreement with the result previously obtained using different normalization criteria for b. Overall, the pH-controlled protein removal method shows a good level of accuracy and is uniform and homogeneous for all of the metabolites, as can be inferred by the small "max" value of a throughout the analytes. Indeed, post-processing approaches that try to extract the peak fingerprint from the measured intensity and the CPMG are inherently affected by the low S/N ratio characterizing the subtler details of individual spectra (shoulders) at low concentrations. In contrast, methods that are based on the physical removal of the serum significantly increase the concentration range that is not affected by accuracy degradation, as can also be deduced from the comparison of the percentage errors returned by different approaches measured at every concentration and for every metabolite (see Fig. 5 in Ref. [21]).

Biological applications

The absolute q-NMR method was tested in three distinct experiments where we (i) compared the phenotype of wild-type and genetically modified cells in cultures, (ii) examined the effect of pharmacological interventions on such cells, and (iii) determined the impact of cell differentiation on the metabolic profile of cells. In the first experiment, the medium of wild-type Hek293 cells was compared with that of cells overexpressing two human cysteine amidases, acid ceramidase (AC) and N-acylethanolamine acid amidase (NAAA). These enzymes were selected because they are structurally related but exert different effects on the replication of Hek293 cells in which they are transfected; AC expression markedly enhances replication, whereas NAAA expression does not [32].

The results reported in Fig. 3A show that both mutant cell lines display substantially elevated glucose uptake and amino acid consumption than do wild-type cells. This effect is likely to reflect the increased metabolic demand imposed by promoter-driven expression of exogenous proteins. In addition, we found that AC-expressing Hek293 cells consumed larger amounts of glutamine and valine compared with either NAAA-expressing or wild-type cells (Fig. 3A). Such a high rate of glutamine metabolism is

Table 4
Comparison of methods for removal of protein signals, square correlation coefficient (R^2), and figure of merit a.

Nutrient	Serum removal		1D–CPMG		Assure Bruker baseline filtering		MestReNova "fitting" algorithm	
	a	R^2	a	R^2	a	R^2	a	R^2
α-Glucose	0.0032	0.9999	0.0937	0.9997	0.2214	0.9994	0.1744	0.9994
β-Glucose	0.0062	0.9999	0.2854	0.9995	0.2642	0.9993	0.1271	0.9991
Histidine	0.0018	0.9997	4.6512	0.9985	1.4114	0.9992	1.3461	0.9959
Phenylalanine	0.0010	0.9993	0.2912	0.9991	1.3648	0.9999	0.5190	0.9996
Tyrosine	0.0004	0.9998	0.6122	0.9983	1.1929	0.9992	0.4243	0.9949
Glutamine	0.0012	1.0000	0.0710	0.9997	2.3420	0.9998	0.2939	0.9997
Isoleucine	0.0035	0.9997	0.4167	0.9889	0.1005	0.9975	0.5777	0.9980
Valine	0.0005	0.9997	0.8238	0.9995	0.0015	0.9959	0.3014	0.9995
Mean	0.0022	0.9998	0.9057	0.9979	0.8635	0.9988	0.4705	0.9983
Max	0.0062		4.6512		2.3420		1.3461	

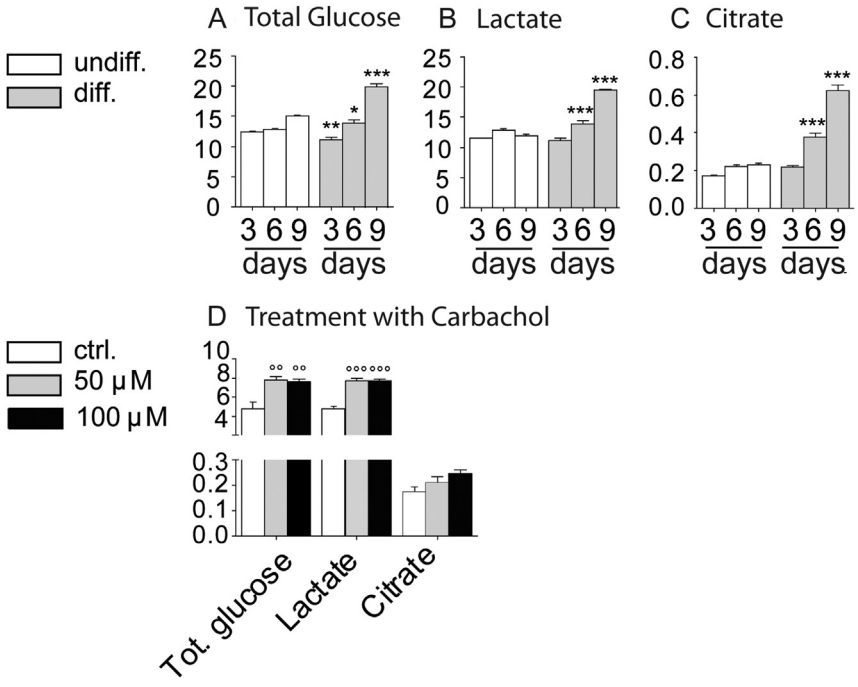

Fig.5. (A–C) Absolute concentration of nutrient uptake and catabolites (mM) in C2C12 cells normalized to the total protein content of the undifferentiated dish sample at each time point. For nutrients (glucose), the absolute value of the difference between the amount measured in cell culture medium and the amount of same nutrient in DMEM without cells is reported. The concentrations of catabolites (lactate and citrate) are reported as measured in cell culture medium. (A) Total glucose uptake. (B) Lactate release. (C) Citrate release. One-way ANOVA followed by all pairwise Tukey's multiple comparison test: $^{***}P < 0.001$, $^{**}P < 0.01$, and $^{*}P < 0.05$ significant versus undifferentiated cells. (D) Treatment with carbachol at doses of 25 and 50 µM analyzed by one-way ANOVA followed by Dunnett's multiple comparison post hoc test versus control (ctrl): $^{\circ\circ\circ}P < 0.001$ and $^{\circ\circ}P < 0.01$. Results are expressed as means ± standard errors ($n = 3–4$). Experiments were repeated twice with similar results.

consistent with recent findings suggesting that highly replicating cancer cells can use glutamine as a source of carbon for Krebs cycle intermediates [33].

Compared with nutrients, products of cell metabolism (i.e., catabolites) are generally released in the medium at low concentration (lactate is an exception). The peaks of these analytes (e.g., 3-methyl-2-oxovaleric acid) are partially covered by protein signals, but they became clearly observable, and thus quantifiable, after serum removal (Fig. 4). Although an improved S/N ratio facilitated the identification of these products via 2D experiments, their identity was confirmed using authentic standards.

Catabolite concentrations appear to depend on the cellular phenotype. Indeed, NAAA-expressing Hek293 cells released in the medium a significantly greater amount of lactate, whereas AC-expressing cells released more alanine and wild-type cells released more 3-methyl-2-oxovaleric acid (Fig. 3A). The significance of these differences was not explored further, but increased alanine excretion in AC-expressing cells might be related to heightened glutamine catabolism [33].

Next, we blocked glycolysis in wild-type and mutant Hek293 cells using the hexokinase inhibitor 3-bromopyruvic acid [34]. We analyzed the cell culture medium 18 h after the addition of the inhibitor (Fig. 3B–E). Treatment with 3-bromopyruvic acid (50 µM) was accompanied by significant decreases in glucose uptake in the three cell lines. By contrast, decreases in lactate release were observed only in wild-type Hek293 cells, confirming the possibility that transfected cells might use another source of carbon for lactate biosynthesis in addition to glucose.

In a second experiment, we differentiated the myoblast cell line C2C12 into myotubes by exposing them to low concentrations of horse serum (2%) [35] (see Fig. S2A and S2B in supplementary material). Nutrient uptake and extracellular metabolite levels were compared with those of undifferentiated C2C12 in the presence of 20% fetal bovine serum (Fig. S2A). Thus, a serum removal step was unavoidable for a meaningful comparison of metabolites between differentiated and undifferentiated cells due to the different serum concentrations in media. Differentiated cells showed a significant time-dependent increase in glucose uptake, and lactate and citrate release (Fig. 5A–C).

By contrast, metabolite concentrations remained substantially constant in undifferentiated cells. After 3 days, proliferating cells consumed significantly higher amounts of glucose (Fig. 5A), but glucose uptake was significantly higher in fully differentiated cells (after 6 days). Correspondingly, lactate release from differentiated cells after 6 days (Fig. 5B) was significantly higher compared with undifferentiated cells. Citrate was always higher in differentiated cells (Fig. 5C).

In a third experiment, we treated differentiated C2C12 myotubes, which express nicotinic cholinergic receptors [36], with the cholinergic agonist carbachol (50 or 100 µM). Agonist exposure resulted in a significant increase in glucose uptake and lactate release (Fig. 5D).

Conclusions

We have developed and validated a new protocol that, after pH-controlled serum protein removal, allows for the absolute quantification of hydrophilic metabolites in cell culture media, using PULCON *q*-NMR, without the employment of any commercial databases or dedicated software. The method, which is simple, inexpensive, and implementable on any type of NMR spectrometer, is highly reliable and, compared with others previously described in the literature, shows the lowest discrepancy from true values, allowing for the quantification of nutrient uptake and release of multiple metabolites irrespective of serum amount, peak shape, and degree of overlap with protein signals. The protocol, applied to

different biological examples, allowed us to quantify with high accuracy several key metabolites released from cells into the medium, even at low concentrations. Considering that protein precipitation is a step widely employed also in high-performance liquid chromatography (HPLC), the same sample may be processed both by NMR and, thanks to the complete sample recovery, by other analytical techniques (e.g., mass spectrometry). The new protocol, therefore, may offer a common analytical platform for the direct comparison of results obtained with different techniques [16,17] and may provide a useful tool for diagnostic and biomarker discovery.

Acknowledgments

L.G. gratefully thanks Francesca Benevelli and Corrado Dallacosta (Bruker Italia), Silvia Mari (MestreLab Research), and Sergio Decherchi for helpful discussion and valuable suggestions.

Appendix A. Supplementary data

Supplementary data related to this article can be found at http://dx.doi.org/10.1016/j.ab.2016.02.009.

References

[1] J.L. Jungnickel, J.W. Forbes, Quantitative measurement of hydrogen types by integrated nuclear magnetic resonance intensities, Anal. Chem. 35 (1963) 938–942.
[2] D.P. Hollis, Quantitative analysis of aspirin, phenacetin, and caffeine mixtures by nuclear magnetic resonance spectrometry, Anal. Chem. 35 (1963) 1682–1684.
[3] M.R. Viant, B.G. Lyeth, M.G. Miller, R.F. Berman, An NMR metabolomic investigation of early metabolic disturbances following traumatic brain injury in a mammalian model, NMR Biomed. 18 (2005) 507–516.
[4] S.K. Bharti, R. Roy, Quantitative ^{1}H NMR spectroscopy, Trends Anal. Chem. 35 (2012) 5–26.
[5] M.J.T. Milton, T.J. Quinn, Primary methods for the measurement of amount of substance, Metrologia 38 (2001) 289–296.
[6] M.E. Dumas, E.C. Maibaum, C. Teague, H. Ueshima, B. Zhou, J.C. Lindon, J.K. Nicholson, J. Stamler, P. Elliott, Q. Chan, E. Holmes, Assessment of analytical reproducibility of ^{1}H NMR spectroscopy based metabonomics for large-scale epidemiological research: the INTERMAP Study, Anal. Chem. 78 (2006) 2199–2208.
[7] W.M. Maniara, A. Cipriano, M.L. Powell, Quantitative analytical methods for the determination of a new hypertension drug, CGS 25462, and its metabolites (CGS 25659 and CGS 24592) in human plasma by high-performance liquid chromatography, J. Chromatogr. B 706 (1998) 287–294.
[8] R.J. Wells, J.M. Hook, T.S. Al-Deen, D.B. Hibbert, Quantitative nuclear magnetic resonance (*q*-NMR) spectroscopy for assessing the purity of technical grade agrochemicals: 2,4-Dichlorophenoxyacetic acid (2,4-D) and sodium 2,2-dichloropropionate (dalapon sodium), J. Agric. Food Chem. 50 (2002) 3366–3374.
[9] G. Wider, L. Dreier, Measuring protein concentrations by NMR spectroscopy, J. Am. Chem. Soc. 128 (2006) 2571–2576.
[10] D.I. Hoult, R.E. Richards, The signal-to-noise ratio of the nuclear magnetic resonance experiment,, J. Magn. Reson. 24 (1976) 71–85.
[11] D.I. Hoult, The principle of reciprocity in signal strength calculations—A mathematical guide, Concepts Magn. Reson. 12 (2000) 173–187.
[12] J.J. Van der Klink, The NMR reciprocity theorem for arbitrary probe geometry, J. Magn. Reson. 148 (2001) 147–154.
[13] I.W. Burton, M.A. Quilliam, J.A. Walter, Quantitative ^{1}H NMR with external standards: use in preparation of calibration solutions for algal toxins and other natural products, Anal. Chem. 77 (2005) 3123–3131.
[14] B.C. Garrido, L.J. de Carvalho, Nuclear magnetic resonance using electronic referencing: method validation and evaluation of the measurement uncertainties for the quantification of benzoic acid in orange juice, Magn. Reson. Chem. 53 (2015) 135–141.
[15] G.A. Nagana Gowda, Y.N. Gowda, D. Raftery, Expanding the limits of human blood metabolite quantitation using NMR spectroscopy, Anal. Chem. 87 (2015) 706–715.
[16] G.A. Nagana Gowda, D. Raftery, Quantitating metabolites in protein precipitated serum using NMR spectroscopy, Anal. Chem. 86 (2014) 5433–5440.
[17] A. Beltran, M. Suarez, M.A. Rodriguez, M. Vinaixa, S. Samino, L. Arola, X. Correig, O. Yanes, Assessment of compatibility between extraction methods for NMR- and LC/MS-based metabolomics, Anal. Chem. 84 (2012) 5838–5844.
[18] A.M. Weljie, J. Newton, P. Mercier, E. Carlson, C.M. Slupsky, Targeted profiling: quantitative analysis of ^{1}H NMR metabolomics data, Anal. Chem. 78 (2006) 4430–4442.
[19] D. Pizzirani, A. Bach, N. Realini, A. Armirotti, L. Mengatto, I. Bauer, S. Girotto, C. Pagliuca, M. De Vivo, M. Summa, A. Ribeiro, D. Piomelli, Benzoxazolone carboxamides: potent and systemically active inhibitors of intracellular acid ceramidase, Angew. Chem. Int. Ed. Engl. 54 (2015) 485–489.
[20] A. Armirotti, E. Romeo, S. Ponzano, L. Mengatto, M. Dionisi, C. Karacsonyi, F. Bertozzi, G. Garau, G. Tarozzo, A. Reggiani, T. Bandiera, G. Tarzia, M. Mor, D. Piomelli, β-Lactones inhibit N-acylethanolamine acid amidase by S-acylation of the catalytic N-terminal cysteine, ACS Med. Chem. Lett. 3 (2012) 422–426.
[21] L. Goldoni, T. Beringhelli, W. Rocchia, N. Realini, D. Piomelli, Absolute nutrient concentration measurements in cell culture media: ^{1}H *q*-NMR spectra and data to compare the efficiency of pH-controlled protein precipitation versus CPMG or post processing filtering approaches, Data Brief (2016) (submitted).
[22] P.S. Wu, G. Otting, Rapid pulse length determination in high-resolution NMR, J. Magn. Reson 176 (2005) 115–119.
[23] H.H. Gadape, K.S. Parikh, Quantitative determination and validation of pioglitazone in pharmaceutical using quantitative nuclear magnetic resonance spectroscopy, J. Chem. Pharm. Res. 3 (2011) 649–664.
[24] T.R. Hoye, B.M. Eklov, T.D. Ryba, M. Voloshin, L.J. Yao, No-D NMR (no-deuterium proton NMR) spectroscopy: a simple yet powerful method for analyzing reaction and reagent solutions, Org. Lett. 6 (2004) 953–956.
[25] A. Shrivastava, V. Gupta, Methods for the determination of limit of detection and limit of quantitation of the analytical methods, Chron. Young Sci. 2 (2011) 21–25.
[26] F. Malz, H. Jancke, Validation of quantitative NMR, J. Pharm. Biomed. Anal. 38 (2005) 813–823.
[27] U. Holzgrabe, B.W. Diehl, I. Wawer, NMR spectroscopy in pharmacy, J. Pharm. Biomed. Anal. 17 (1998) 557–616.
[28] Y. Wang, M.E. Bollard, H. Keun, H. Antti, O. Beckonert, T.M. Ebbels, J.C. Lindon, E. Holmes, H. Tang, J.K. Nicholson, Spectral editing and pattern recognition methods applied to high-resolution magic-angle spinning ^{1}H nuclear magnetic resonance spectroscopy of liver tissues, Anal. Biochem. 323 (2003) 26–32.
[29] C.A. Daykin, P.J. Foxall, S.C. Connor, J.C. Lindon, J.K. Nicholson, The comparison of plasma deproteinization methods for the detection of low-molecular-weight metabolites by ^{1}H nuclear magnetic resonance spectroscopy, Anal. Biochem. 304 (2002) 220–230.
[30] J.A. Aguilar, M. Nilsson, G. Bodenhausen, G.A. Morris, Spin echo NMR spectra without J modulation, Chem. Commun. 48 (2012) 811–813.
[31] V. Gallo, N. Intini, P. Mastrorilli, M. Latronico, P. Scapicchio, M. Triggiani, V. Bevilacqua, P. Fanizzi, D. Acquotti, C. Airoldi, F. Arnesano, M. Assfalg, F. Benevelli, D. Bertelli, L.R. Cagliani, L. Casadei, F. Cesare Marincola, G. Colafemmina, R. Consonni, C. Cosentino, S. Davalli, S.A. De Pascali, V. D'Aiuto, A. Faccini, R. Gobetto, R. Lamanna, F. Liguori, F. Longobardi, D. Mallamace, P. Mazzei, I. Menegazzo, S. Milone, A. Mucci, C. Napoli, T. Pertinhez, A. Rizzuti, L. Rocchigiani, E. Schievano, F. Sciubba, A. Sobolev, L. Tenori, M. Valerio, Performance assessment in fingerprinting and multi component quantitative NMR analyses, Anal. Chem. 87 (2015) 6709–6717.
[32] N. Realini, C. Solorzano, C. Pagliuca, D. Pizzirani, A. Armirotti, R. Luciani, M.P. Costi, T. Bandiera, D. Piomelli, Discovery of highly potent acid ceramidase inhibitors with in vitro tumor chemosensitizing activity, Sci. Rep. 3 (2013) 1035.
[33] R.J. DeBerardinis, A. Mancuso, E. Daikhin, I. Nissim, M. Yudkoff, S. Wehrli, C.B. Thompson, Beyond aerobic glycolysis: transformed cells can engage in glutamine metabolism that exceeds the requirement for protein and nucleotide synthesis, Proc. Natl. Acad. Sci. U. S. A. 104 (2007) 19345–19350.
[34] H. Pelicano, D.S. Martin, R.H. Xu, P. Huang, Glycolysis inhibition for anticancer treatment, Oncogene 25 (2006) 4633–4646.
[35] M.A. Lawson, P.P. Purslow, Differentiation of myoblasts in serum-free media: effects of modified media are cell line-specific, Cells Tissues Organs 167 (2000) 130–137.
[36] S. Oikawa, A. Mano, M. Iketani, Y. Kakinuma, Nicotinic receptor-dependent and -independent effects of galantamine, an acetylcholinesterase inhibitor, on the non-neuronal acetylcholine system in C2C12 cells, Int. Immunopharmacol. 29 (2015) 31–35.